**swiss*nuclear*: PEGASOS Refinement Project:
SP2 – Ground Motion Characterization**

Contract no. PMT-VT-1032

Seismic Shear Wave Velocity Determination and Hybrid Seismic Survey at the SED-Station SLE (Schleitheim)

Date of Field Data Acquisition 11th December 2008

Revised Report

Client

swiss*nuclear*
Project PRP
Frohburgstrasse 17
4601 Olten

Contractor

GeoExpert ag
Seismic Prospecting
Ifangstrasse 12b
P.O. Box 451
8603 Schwerzenbach

8603 Schwerzenbach, 24th March 2009

INDEX

1 INTRODUCTION

1.1 Survey objectives

The seismic survey's main task is to provide information about the distribution function of the shear wave velocities in the depth interval of the uppermost 30 m along a 100 m long seismic profile.

Additionally, the following objectives are to be met:
- the mapping of the topography of the rock face, i.e. the thickness of the Quaternary deposits;
- the determination of the thickness of the weathered zone and its degree of decompaction at the bedrock surface;
- a general view of geological structures.

1.2 The choice of the appropriate surveying methods

Several methods are available for deriving the s-wave velocity distribution in the subsurface at any given position:
- in-situ measurement by down-hole or crosshole seismic surveying;
- shear-wave refraction tomography profiling;
- dispersion analysis of surface waves (MASW; **M**ultiple channel **A**nalysis of **S**urface **W**aves)

The surveys are to be carried out at, or as close as possible near some 20 SED earth quake monitoring stations in Switzerland. Ideally, the surveys are to be conducted on two orthogonal profiles in order to derive at their point of intersection a robust 1D s-wave velocity distribution function by correlation. To this end, the methods of MASW and shear-wave refraction tomography profiling are to be combined.

The results are to include the following fundamental parameters $v_{s,5}$, $v_{s,10}$, $v_{s,20}$, $v_{s,30}$, $v_{s,40}$, $v_{s,50}$, $v_{s,100}$ are to be calculated, also an error estimation of all values.

The data acquired for the MASW method are to be subjected to complementary **p-wave hybrid seismic data processing** in order to image the geological structures.

2 FIELD DATA ACQUISITION PARTICULARS

2.1 Time Schedule

Date	Time	Activities / remarks
11.12.2008	0630 - 0745	traveling from Schwerzenbach
	0745 - 0800	site reconnaissance
	0815 - 1015	lay-out of recording spread
	1030 - 1110	compressional wave data recording
	1200 - 1310	shear wave data recording
	1310 - 1345	retrieval of the recording spread
	1445	departure from site

2.2 Summary of Data Acquisition Parameters

Compressional Wave Data Acquisition

# of active channels	96
geophone type	4.5 Hz natural frequency, vertical velocimeter
receiver station spacing	1.0 m
# of geophones/station	1
source point spacing	3.0 m
source type	vertical hammer (6 kg) striking on a horizontal metal plate
sampling rate	500 µs
recording time	2048 ms
field filters	0.5 Hz LC, anti-alias
# of field records	41

Shear Wave Data Acquisition

# of active channels	48
geophone type	10 Hz natural frequency, horizontal velocimeter
receiver station spacing	2.0 m
# of geophones/station	1
source point spacing	4.0 m to 6.0 m
source type	horizontal hammer (6 kg) striking horizontally at a metal-plated wooden beam anchored to the ground by means of 20 cm long spikes
sampling rate	500 µs
recording time	512 ms
field filters	2 Hz LC, anti-alias
# of field records	40 at 20 positions

Fig. 2.1: S-wave data acquisition: striking at the metal-plated wooden beam with the hammer. In front: line and jumper cables.

2.3 Composition of Seismic Field Crew

Personnel

Keller Lorenz	dipl. Natw. ETH, party chief, geophysicist
Walter Frei	dipl. Natw. ETH, seismic observer, geophysicist
Fiseli Jochen	dipl. Geologe, Uni Freiburg i. Br., activation of seismic source

Equipment

96	vertical geophones 4.5 Hz
48	horizontal geophones 12 Hz
6	seismic cables
1	seismic acquisition system Summit Compact, 96 channels
1	laptop computer for data acquisition
3	walkie-talkies
1	hammer 6 kg
1	steel plate
1	metal-plated wooden beam
1	van (FIAT Ducato 4x4)

2.4 Location

The seismic monitoring station SLE (Schleitheim) is situated on the top of a mesozoic (Keuper) sediment ridge(limestone and marl) in northern Switzerland, canton of Schaffhausen. The station is located directly in a abandoned quarry.
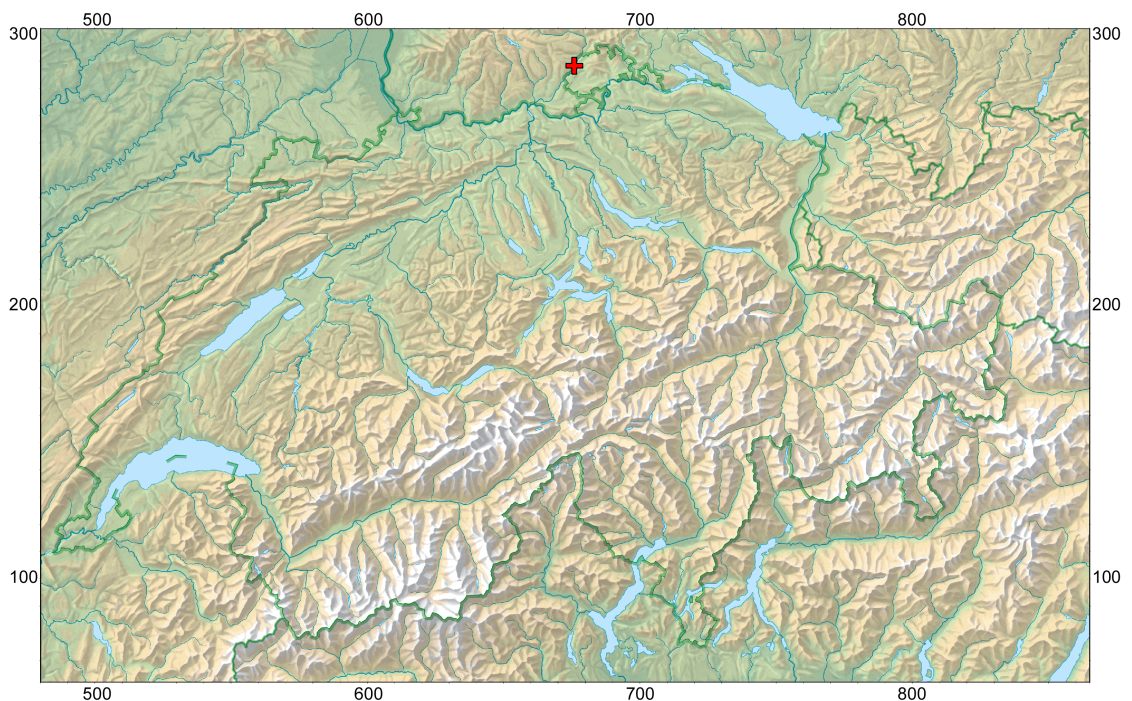
Fig. 2.2:   The red cross marked seismic monitoring station SLE (Schleitheim) is located in Schaff-hausen's mesozoic sediments (Keuper).
(map: geodata @ swisstopo).

2.5 Recording Conditions and Line Setup

Light snowfall prevailed throughout the field data recording period. The ground was covered with 20 cm of snow.

In general, the data quality obtained under the prevailing conditions is to be rated as very good.

Because of terrain difficulties and due to impenetrable dense brush off the amenable dirt road leading to the monitoring station, no data could be acquired on a second line intersecting line 09SN_14SLE-**1** and being within less than 70 m from the monitoring station.

During the data recording work, it became apparent that the geological conditions change rapidly with increasing southward distance from the monitoring station. At the southern end of line 1, near the main access road, along which an alternative second line could be placed, the bedrock surface was found to be situated at a considerable depth, as compared to the outcropping bedrock at locations closer to the monitoring station. Since surveying at two sites with different geological settings produces inconsistencies of the results, it was decided not to record any data along the main access road.

Coordinates Line 09SN_SLE-1:
Station 101: 679.054 / 290.898
Station 192: 679.017 / 290.986

nearest profile station no.: 172

Legend

SED station

seismic line

0   10   20   30   40   50m
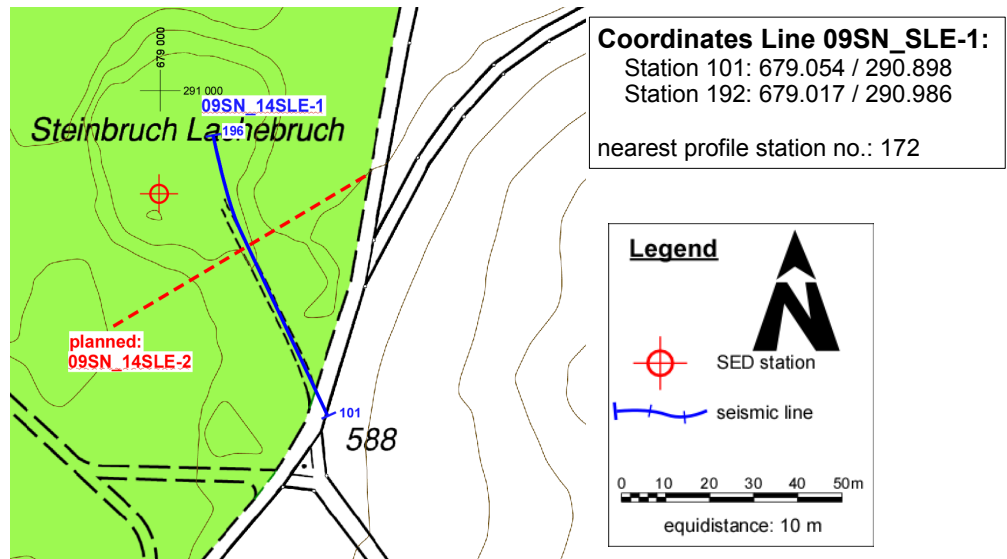
equidistance: 10 m

Fig. 2.3:   *Situation map with the trace of seismic profile 09SN_14SLE-1. The profile 09SN_14SLE-2 was originally planned but not recorded due to terrain difficulties. (background map: © GIS canton of Schaffhausen.)*

3 SEISMIC DATA PROCESSING AND IMAGING OF THE RESULTS

3.1 General Remarks

- Picking the first break time arrivals of shear wave data, the system **ReflexW** of Sandmeyer Scientific Software, Karlsruhe DE was used (www.sandmeyer-geo.de).

- For the shear and compressional wave refraction seismic evaluation the package **RAYFRACT** by Intelligent Resources Ltd., Vancouver CAN, was used. The system features the technique of diving wave tomography (www.rayfract.com).

- The system **SPW** (**S**eismic **P**rocessing **W**orkshop) of Parallel Geoscience Corporation, Austin US-TX, was used for reflection seismic data processing (www.parallel-geo.com).

- Data processing of surface waves (MASW processing) was conducted with the software package **SurfSeis** V2.0 of Kansas Geological Survey in Lawrence US-KS.

A detailed description of the various surveying methods will be included in the general summary report.

3.2 Shear Wave Refraction Tomography

3.2.1 Reformatting and field geometry assignment

After reformatting the field data into the ReflexW format the field geometry is applied.

3.2.2 First break time picking

At each shot position, two seismic records were acquired in both activation directions. These two records are displayed superimposed with different colors on each other in Fig 3.2a together with the manually determined first arrival time picks.
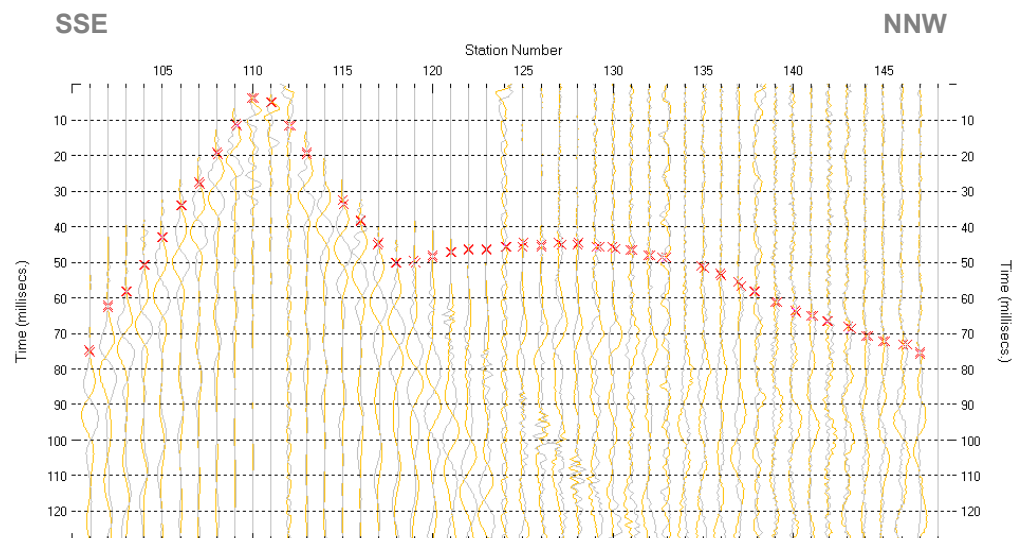

Fig. 3.2a: *High quality dual field record showing at each station the s-wave traces with opposing polarities in different colors. The manually picked s-wave refraction arrivals at each receiver station are marked with an* **x**.
The station spacing is 2 m; profile station 101 = profile meter 1; profile station 148 = profile meter 95.

SSE   NNW
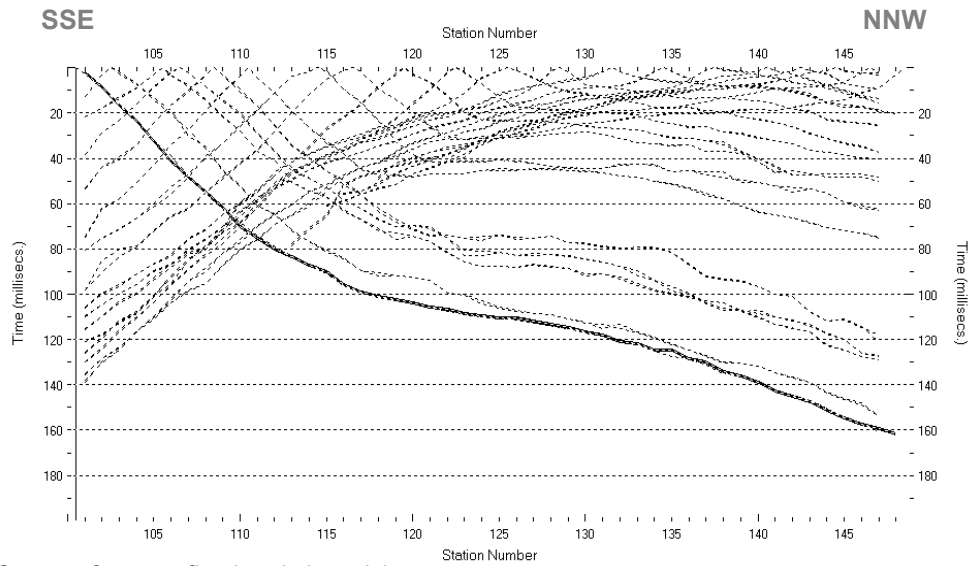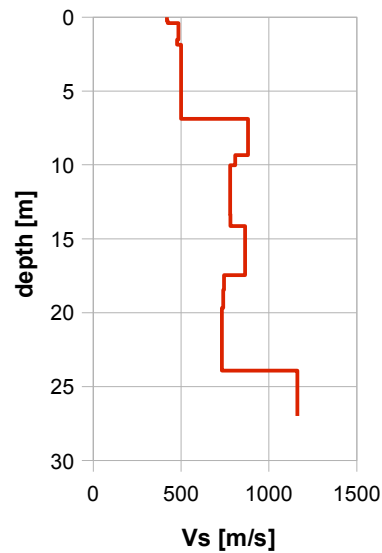
Fig. 3.2b: Curves of s-wave first break time picks.
The station spacing is 2 m; profile station 101 = profile meter 1; profile station 148 = profile meter 95.

3.2.3   Analytical Determination of Refraction Velocities

An initial 1D-velocity function (averaged 1D velocity-depth profiles derived by the Delta-t-V method, see Tab. 3.2a) is determined in the 3-dimensional time-offset-CMP-domain from all first break arrival time curves in the 3-dimensional time-offset-CMP-domain (see. Fig. 3.2c).

Depth [m]	Vs [m/s]
0.0	420
0.3	424
0.4	485
1.5	478
1.9	500
6.9	881
9.3	809
10.0	780
11.9	779
13.3	781
14.1	864
17.5	745
18.5	740
19.7	732
23.9	1162

Tab. 3.2a: Initial 1D s-wave velocity function derived from real data. The plotted values are mean values between profile meters 70 and 80.
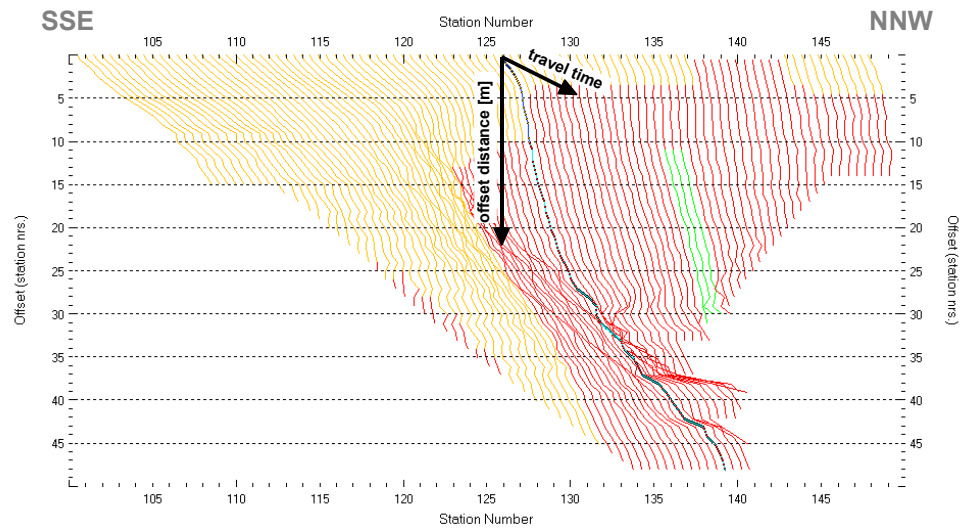
Fig. 3.2c: 3-dimensional distance-travel time diagrams at the mid-points between source points and receiver stations are instrumental when using the analytical CMP derivation of the initial velocity field.
The horizontal axes are the along the CMP positions and the travel time respectively, the vertical axis denotes the offset distance between source and receiver positions. The station spacing is 2 m, profile station 101 = profile meter 1; profile station 148 = profile meter 95. The colors represent different velocity layers.

3.2.4 Tomographic inversion of the velocity gradient field by iterative modeling

The velocity field is iteratively refined by the subsequent Wavepath Eikonal Traveltime (WET) tomographic inversion process. The inversion results are portrayed in Fig. 3.2d as a gridded velocity contour section and in Fig. 3.2e as a ray path density section.
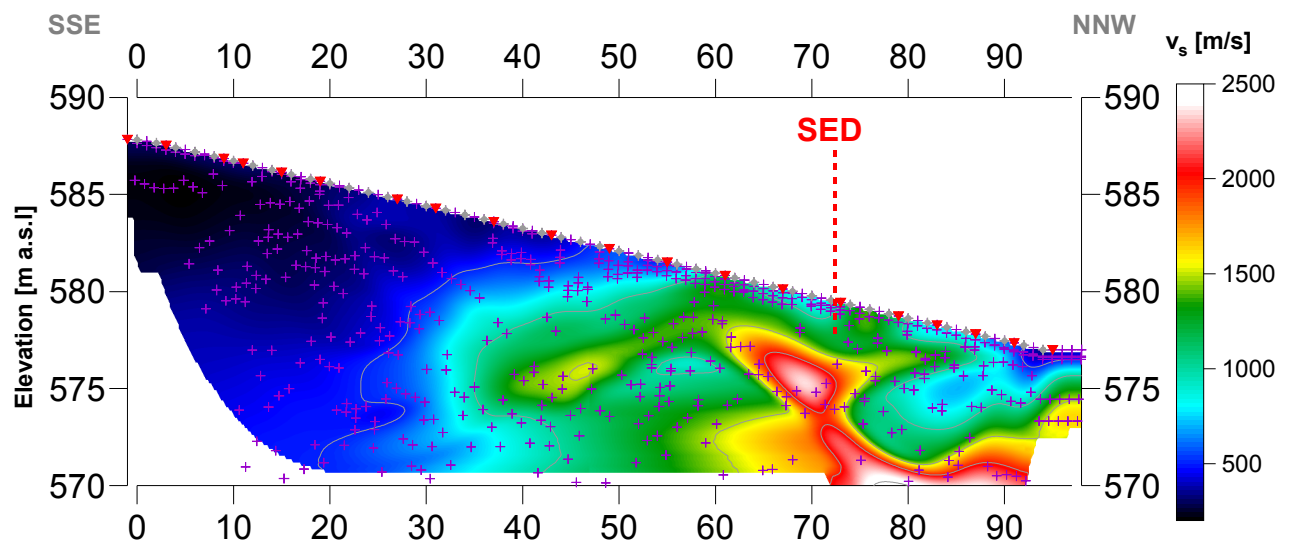
Fig. 3.2d: Shear wave velocity field of the profile. Red/white colors denote solid rock, blue/black colors point to unconsolidated sediments and soil.
Vertical axis: elevation [m a.s.l]; horizontal axis: profile meter; color encoded scale: v_s [m/s]; vertical exaggeration: 2:1; gray diamonds: receiver positions; red triangles: source positions; magenta crosses: positions of determined velocity values deriving the initial velocity model. The station spacing is 2 m, profile meter 1 = profile station 101, profile meter 95 = profile station 148.

Fig. 3.2e: Shear wave ray path density along the seismic profile. Red/white colors indicate high velocity contrasts (usually at the bedrock surface), blue/black colo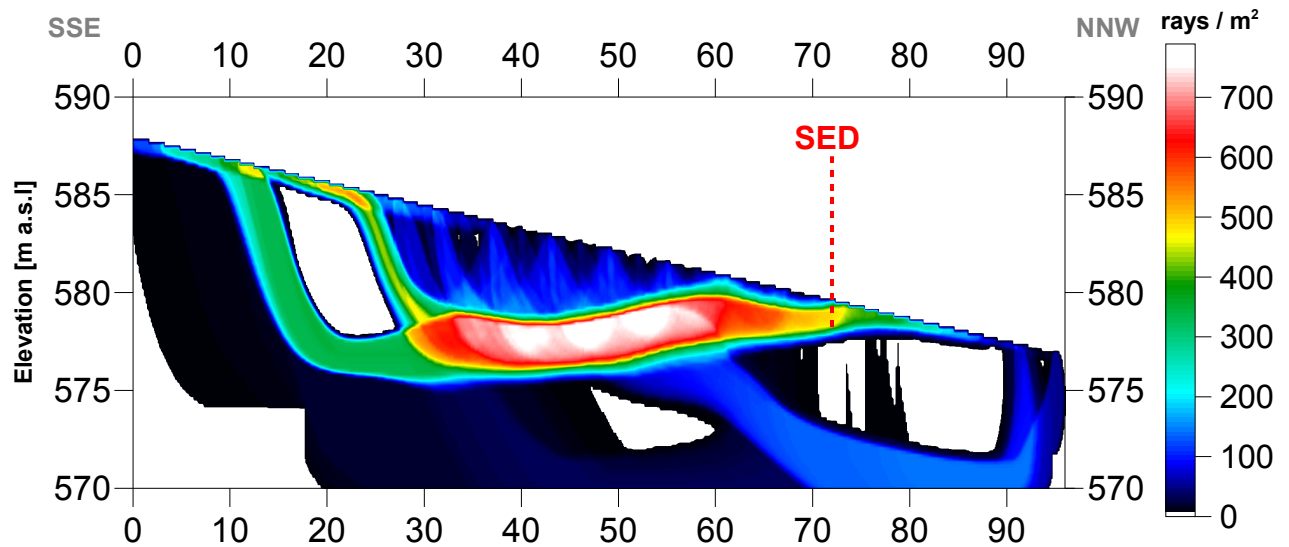rs denote low coverage areas. Vertical axis: elevation [m a.s.l]; horizontal axis: profile meter; color encoded scale: ray paths per m²; vertical exaggeration: 2:1. The station spacing is 2 m, profile meter 1 = profile station 101, profile meter 95 = profile station 148.

Depth [m]	Vs [m/s]
0.0	783
0.5	904
1.0	1173
1.5	1191
2.1	1214
2.6	1273
3.1	1455
3.7	1631
4.2	1663
4.7	1574
5.3	1453
5.8	1384
6.3	1383
6.9	1466
7.4	1595
7.9	1746
8.5	1925
9.0	2117
9.5	2342
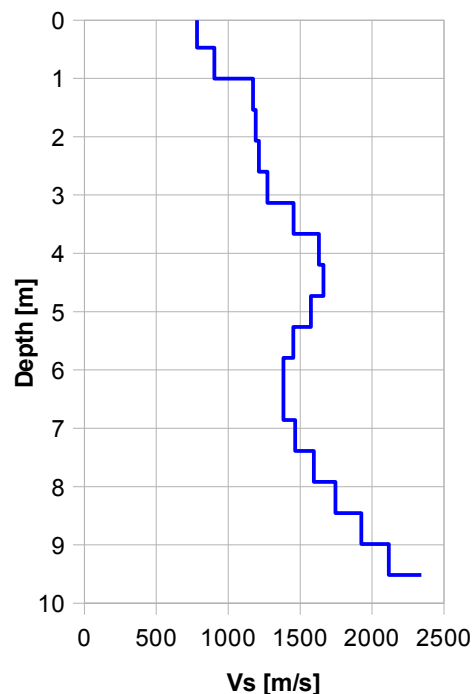
Tab. 3.2b: Final 1D s-wave velocity model derived from real data (horizontal average of all values) at a position most similar to the geological setting at SED station between profile meters 70 and 80.

The attained depth of investigation being limited to 10 m is to be attributed to the method inherent constraining factor of critically refracted waves along the shallow bedrock surface, combined with the insufficient length of the lay-out spread for recording long offset data needed for deeper penetration.

3.3 MASW Processing

3.3.1 Reformatting and field geometry assignment

The data preparation steps for the dispersion analysis include
- the assignment of the field acquisition geometry
- the selection of suitable offset ranges (=arrays) between 10 m and 50 m for dispersion, and the splitting of the field records in forward and reverse shooting direction data sets
- the reformatting of the data into the specific KGS format

X - - ... - - o-o-o-...-o-o-o (forward shooting or so-called PLUS direction)
respectively
o-o-o-...-o-o-o - - ... - - X (reverse shooting or so-called MINUS direction).

where   **X** = shot position
              o = receiver station
              - = 1.0 m offset

The active array used at SED-station SLE were the receivers in the shot offset range between 10 and 50 m.

3.3.2 Calculating the dispersion image (overtone)

The result of dispersion analysis is the color encoded acoustic energy distribution the phase velocity - frequency plane (see Fig. 3.3a and b).
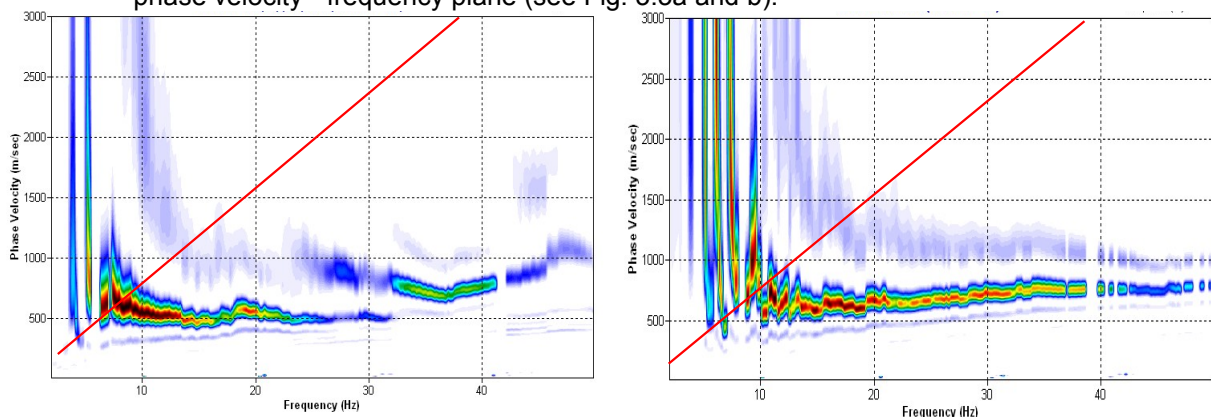

Fig. 3.3a: Dispersion image of good quality data (left) from midpoint station 142 as found on 70% and of fair quality data (right) from midpoint station 152 representing about 30% of the MASW dataset of profile 09SN_14SLE-1 (left).
Horizontal axis: frequency from 3 to 50 Hz; vertical axis: phase velocity from 200 to 3000 m/s; color code: colors from white (no energy) to blue - green - yellow - red - black point to increasing energy amplitude values; red line: high resolution beam-forming curve for v_{max}.

3.3.3 Analysis of the dispersion image

In the dispersion graphs as calculated in section 3.3.2 above, the curves joining the amplitude peaks of the fundamental modes are determined either by subjective inspection or in a semi-automated manner. On datasets with poorly defined amplitude peaks or with a highly irregular alignment of the peaks, the danger of obtaining improbable or wrong results is real and can only be mitigated by the processing experience and the a-priori knowledge of the geological setting by the geophysicist responsible for the data evaluation.
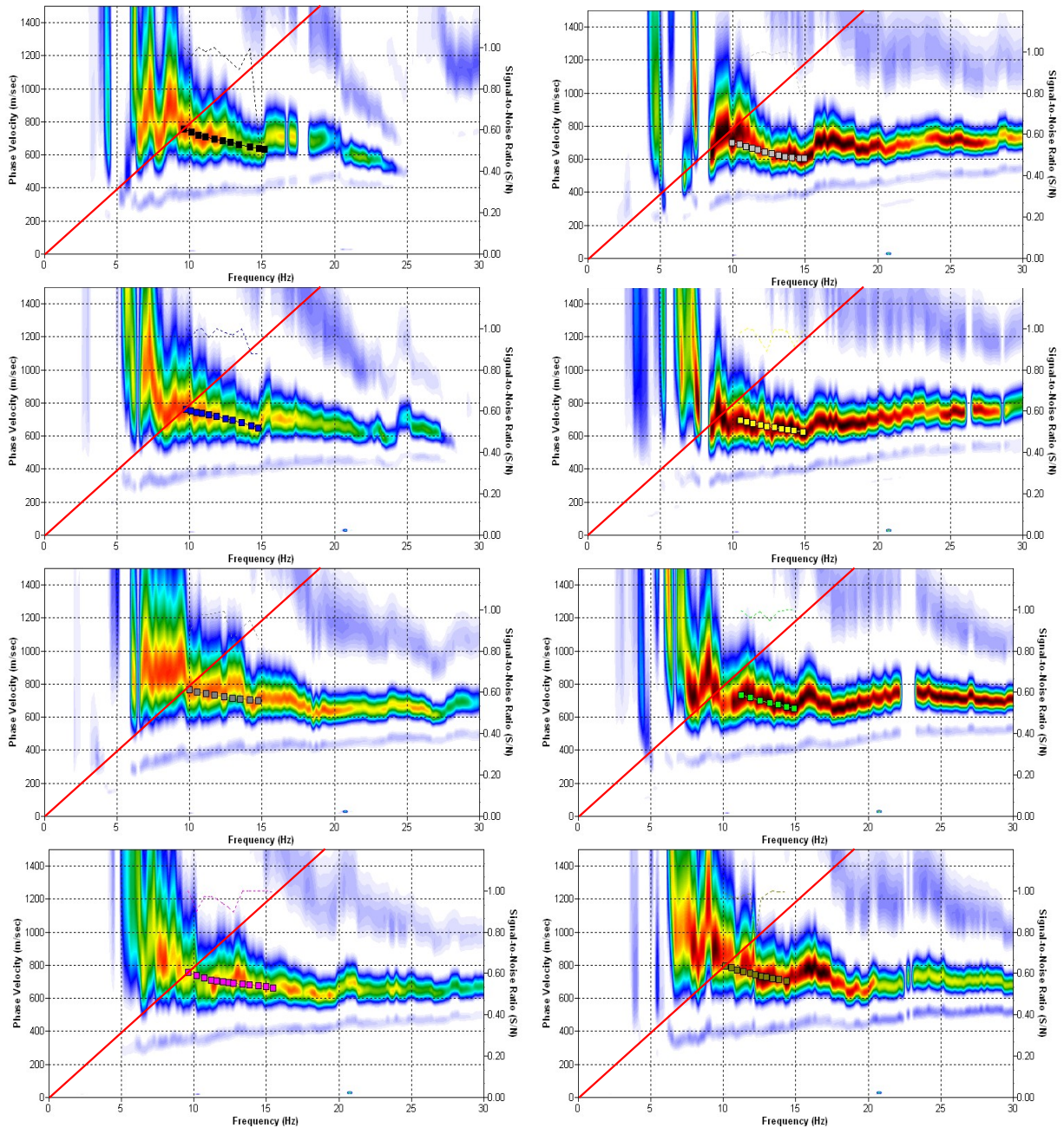
Fig. 3.3b: For the shear wave velocity profile at SED Station SLE most relevant manually picked disper-
sion images. The dispersion curves (squares) following generally the high energy peaks by
joining the peaks of maximum energy. Note that 'higher modes' may at times produce higher
energy peaks than the fundamental mode required for analysis.
dotted fine line: signal-noise ratio for the designated f-v_{ph} – value.
red line: high resolution beam-forming curve for v_{max}.
1st row: left: station 159 @ PLUS direction; *right:* station 160 @ MINUS direction
2nd row: left: station 162 @ PLUS direction; *right:* station 163 @ MINUS direction
3rd row: left: station 164 @ PLUS direction; *right:* station 166 @ MINUS direction
4th row: left . station 168 @ PLUS direction; *right:* station 169 @ MINUS direction

3.3.4 Inversion of dispersion curves resulting in a 1D shear wave velocity distribution

Inversion of the extracted dispersion curves was performed using the algorithm described by Xia et al. (1999).

The inversion process is started by setting the maximum depth (z_{max}) to be in the order of 30% of the largest wavelength for an initial model consisting of 10 layers of equal thicknesses. For all 10 layers, the Poisson's ratio is assumed to be 0.4 and the rock/soil density is fixed at 2.0 g/cm^3. The inversion process is concluded either after twelve iterations or when the convergence condition of an RMS-error of less than 3 m/s (phase velocity) is met.
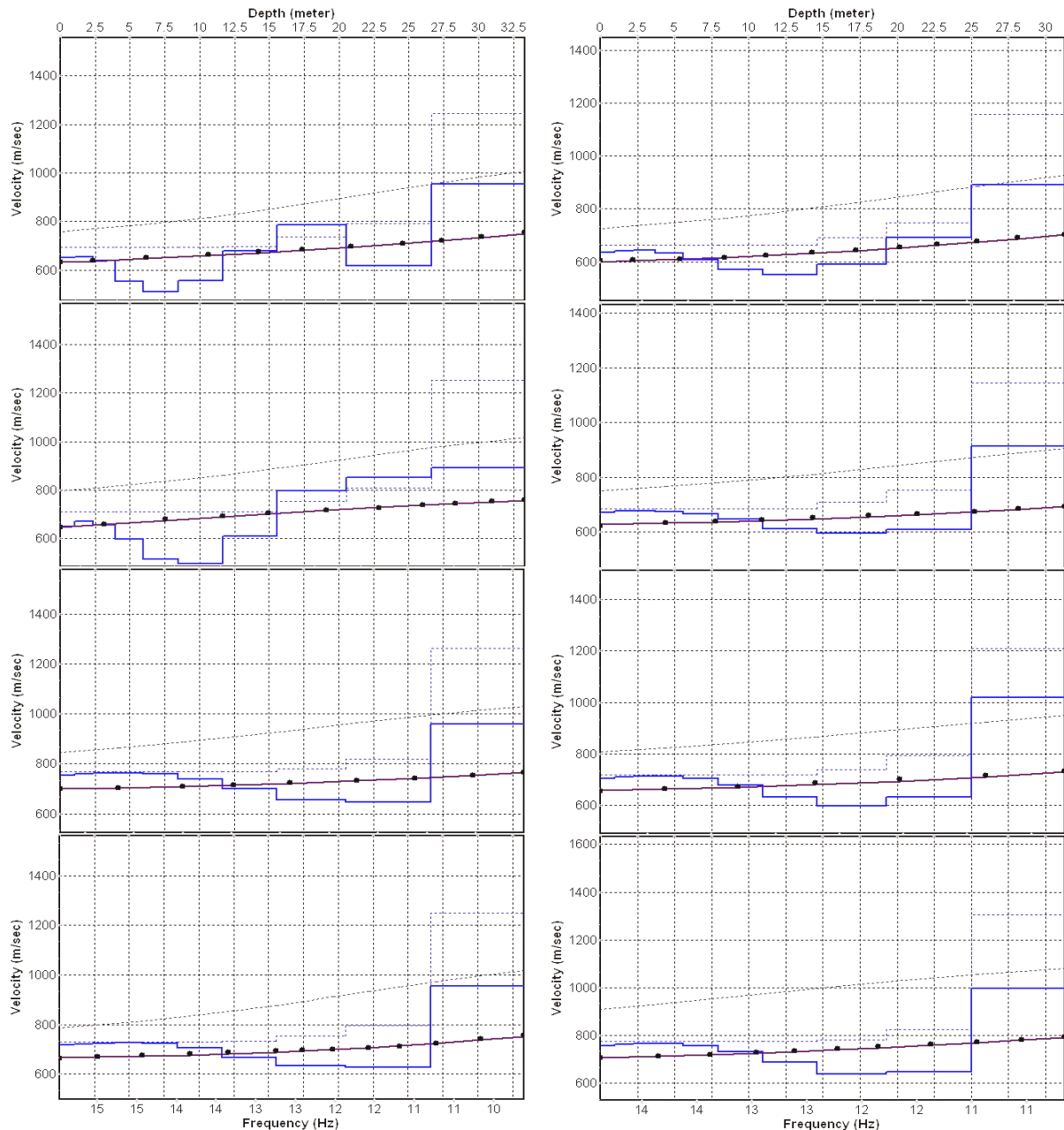
Fig. 3.3c: **brown**: Inversion of dispersion curve (dots) resp. of the modeled dispersion curve (dotted line: initial model; continuous line: end model). Horizontal axis: frequency Hz, vertical axis: v_s.
blue: 10-layer-model (dotted: initial model, continuous line: final model). Horizontal axis: depth, vertical axis: phase velocity resp. v_s).
1st row: left: station 159 @ PLUS direction; right: station 160 @ MINUS direction
2nd row: left: station 162 @ PLUS direction; right: station 163 @ MINUS direction
3rd row: left: station 164 @ PLUS direction; right: station 166 @ MINUS direction
4th row: left . station 168 @ PLUS direction; right: station 169 @ MINUS direction

To compare these dispersion curves with the measurements done by the SED crew, the following 2 records are shown here.
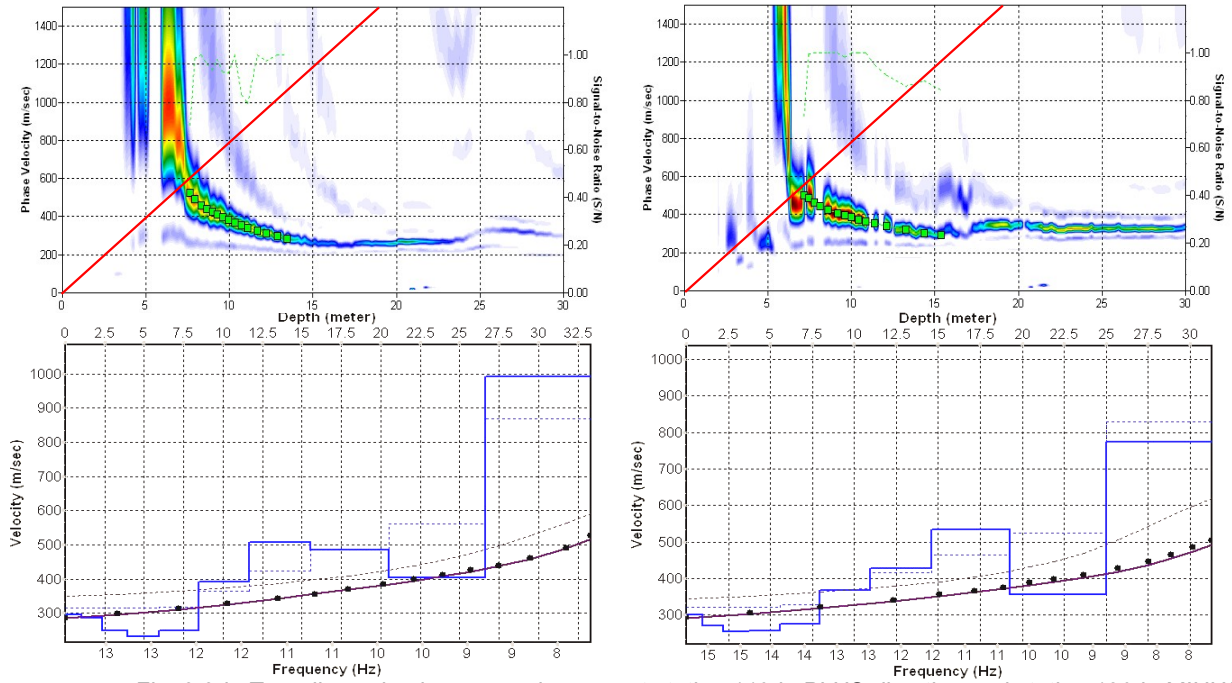

Fig. 3.3d: Top: dispersion images and curves at station 119 in PLUS direction and station 120 in MINUS direction to compare with the SED own measurements; dotted fine line: signal-noise ratio for the designated f-v_{ph} – value. Red line: high resolution beam-forming curve for v_{max}.
Bottom: Inversion of dispersion curve at the same stations; **brown**: inversion of dispersion curve; **blue**: 10-layer-model. Horizontal axis: depth, vertical axis: phase velocity resp. v_s.

Fig. 3.3e: Top: dispersion images of an over-all array (all 96 recorded traces from 10 to 206 m offset) in PLUS (left) and MINUS (right) direction; dotted fine line: signal-noise ratio for the designated f-v_{ph} – value. Red line: high resolution beam-forming curve for v_{max}.
Below: The two respective inversion results; **brown**: inversion of dispersion curve; **blue**: 10-layer-model. Horizontal axis: depth, vertical axis: phase velocity resp. v_s.
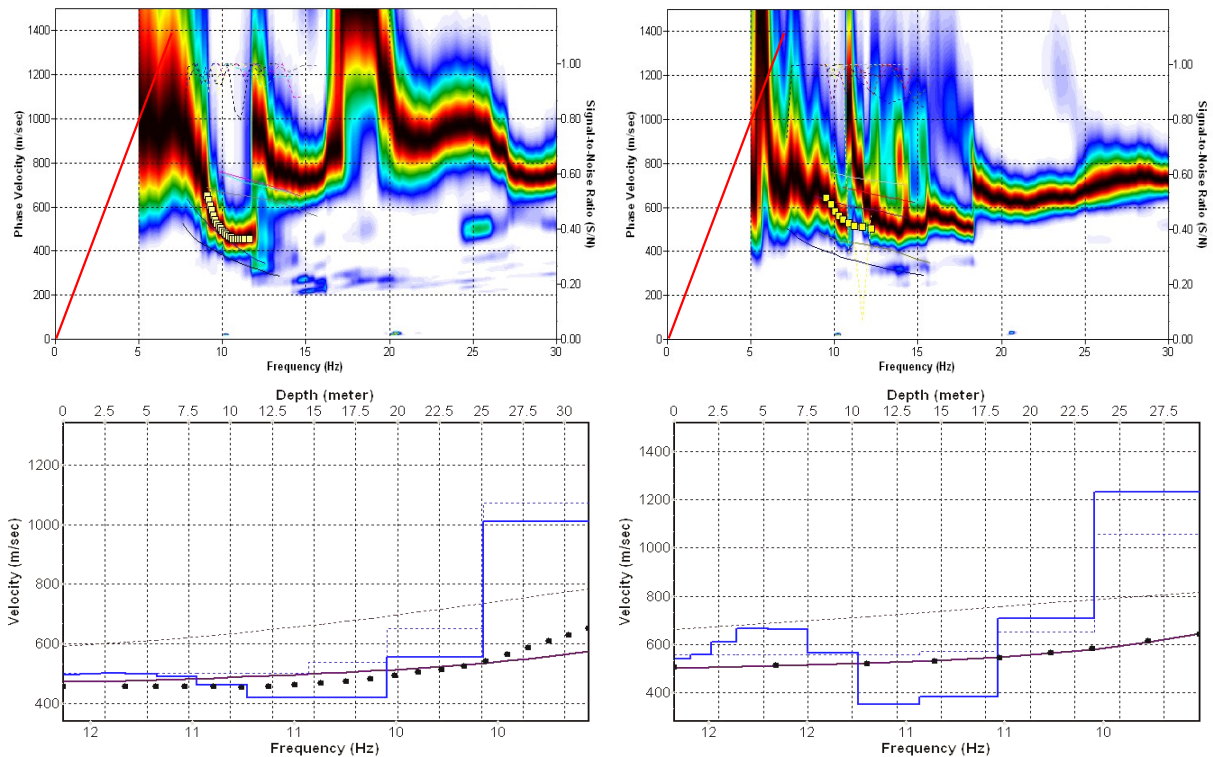
3.3.5 Gridding and plotting of 2D v$_s$-velocity field

By assembling the 1D v$_s$ - depth functions from all stations the final 2D v$_s$-field is derived using a Kriging gridding procedure as portrayed in Fig. 3.3f below:
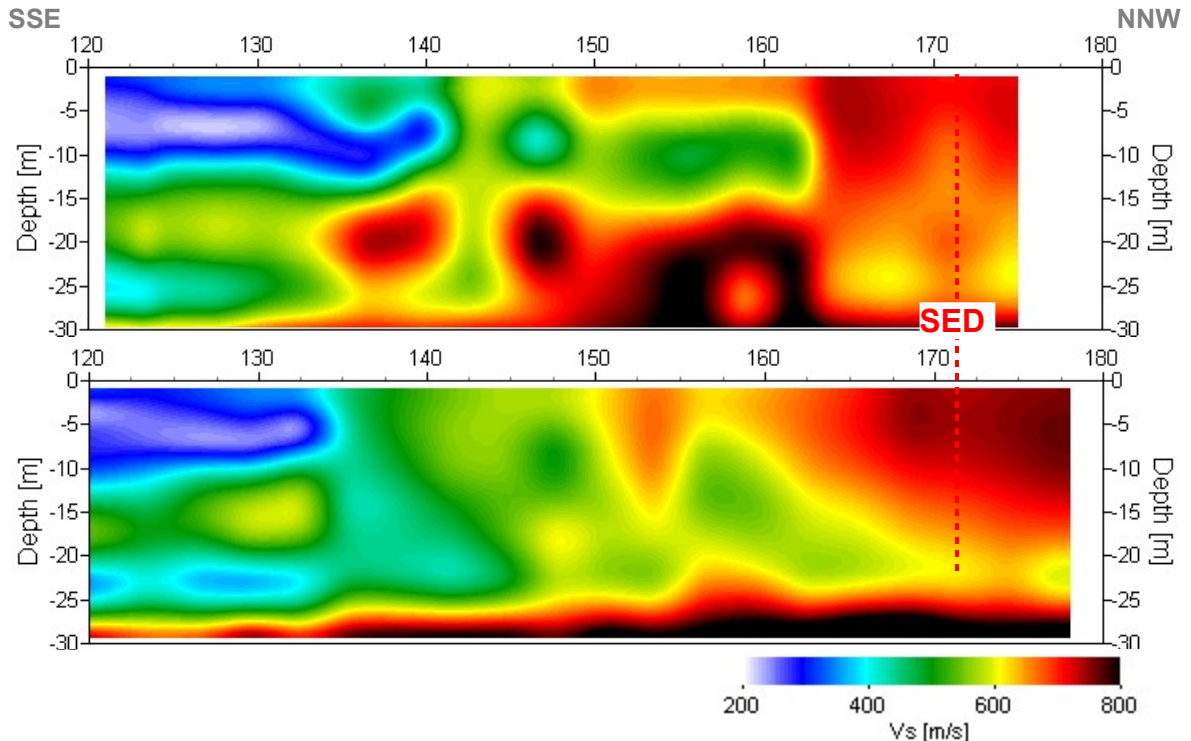

Fig. 3.3f: PLUS- (above) and MINUS- (below)-MASW-processed shear wave velocity fields. Color scale from 200 m/s (white) over 300 m/s (blue), 500 m/s (green), 600 m/s (yellow) and 700 m/s (red) to 800 m/s (black).
The station spacing is 1 m; profile station 120 = profile meter 19; profile station 180 = profile meter 79.

3.3.6 Calculation of the average shear wave velocity

To calculate a representable shear-wave velocity-depth function at SED station, all computed 1D-v$_s$-depth functions between seismic profile station 160 and 170 – that are four profiles in each direction – are averaged (non-weighted mean values). This sector was choiced because of field observations during data acquisition. Another criteria was, that in both directions, at least four dispersion curves exist to invert. The v$_s$-depth-function is shown in Tab. 3.3a.

Depth [m]	Vs- [m/s]	Vs+ [m/s]	Vs [m/s]
0	693	694	694
1.0	697	701	699
2.3	700	695	697
3.8	697	660	678
5.8	683	626	655
8.2	657	625	641
11.3	621	664	642
15.1	606	718	662
19.9	645	686	666
25.8	955	939	947
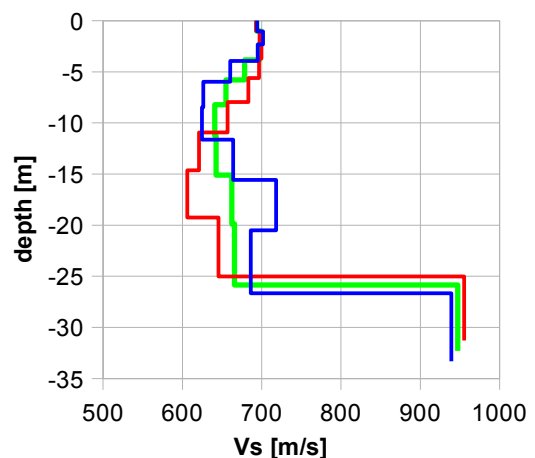
Tab. 3.3a: Averaged v$_s$ - depth function at the SED station SLE. Blue line: MASW-'PLUS' processing, red line: MASW-'MINUS' processing; green line: average of PLUS- and MINUS-functions.

To compare the data with the former SED own measurements, the v$_s$-depth functions from inverted inversion curves at the most southern part (profile station 120, Fig. 3.3d) are shown in Tab. 3.3b.

| Depth [m]	Vs- [m/s]	Vs+ [m/s]	Vs [m/s]
1.0	299	296	298
2.3	270	286	278
3.8	254	250	252
5.8	257	233	245
8.2	274	248	261
11.3	366	392	379
15.1	428	507	467
19.9	533	484	509
25.8	356	404	380
32.3	773	992	883
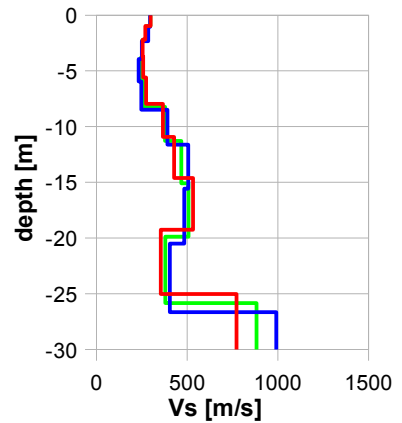
Tab. 3.3b: *The computed v$_s$-depth functions at profile station no. 119/120 are given to compare with the former SED measurements. The belonging dispersion curves are shown in Fig. 3.3d.*

The inversion of the two 100 m array dispersion curves (Fig. 3.3e) data (10 to 106 m offset) are given in Tab. 3.3c.

Depth [m]	Vs- [m/s] over all	Vs+ [m/s] over all	Vs [m/s] over all	Vs [m/s] 10-50
0.9	538	497	517	694
2.1	558	499	529	699
3.6	610	501	555	697
5.5	666	500	583	678
7.8	662	489	575	655
10.6	564	462	513	641
14.2	351	418	385	642
18.8	380	420	400	662
24.4	706	555	631	666
30.5	1234	1010	1122	947
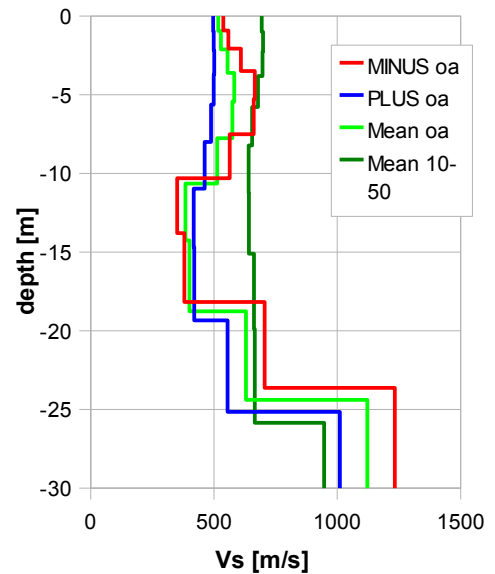
Tab. 3.3c: *v$_s$-depth function from the 100 m-array record analyses (see Fig. 3.3e) and the for the SED station significant values from the analyses ot the 40 m-array records (last column, from Tab. 3.3c).*
red line: over-all-offset analysis MINUS direction.
blue line: over-all-offset analysis MINUS direction.
light green line: mean of both over-all-offset analysis MINUS and PLUS direction.
dark green line: mean of v$_s$-values from analysis of 10..50 m offset records.

3.3.7 Calculation of the shear wave velocity scalars $v_{s,5}$, $v_{s,10}$, ...

The parameters $v_{s,5}$, $v_{s,10}$, $v_{s,20}$, $v_{s,30}$, $v_{s,40}$, $v_{s,50}$ represent the average shear wave velocities in the depth interval from terrain down to to the respective depths and are determined from the formula

$$v_{s,n} = \frac{\sum_{i=1}^{n} d_i}{\sum_{i=1}^{n} d_i/v_{si}}$$

with:

d_i = thickness of layer i
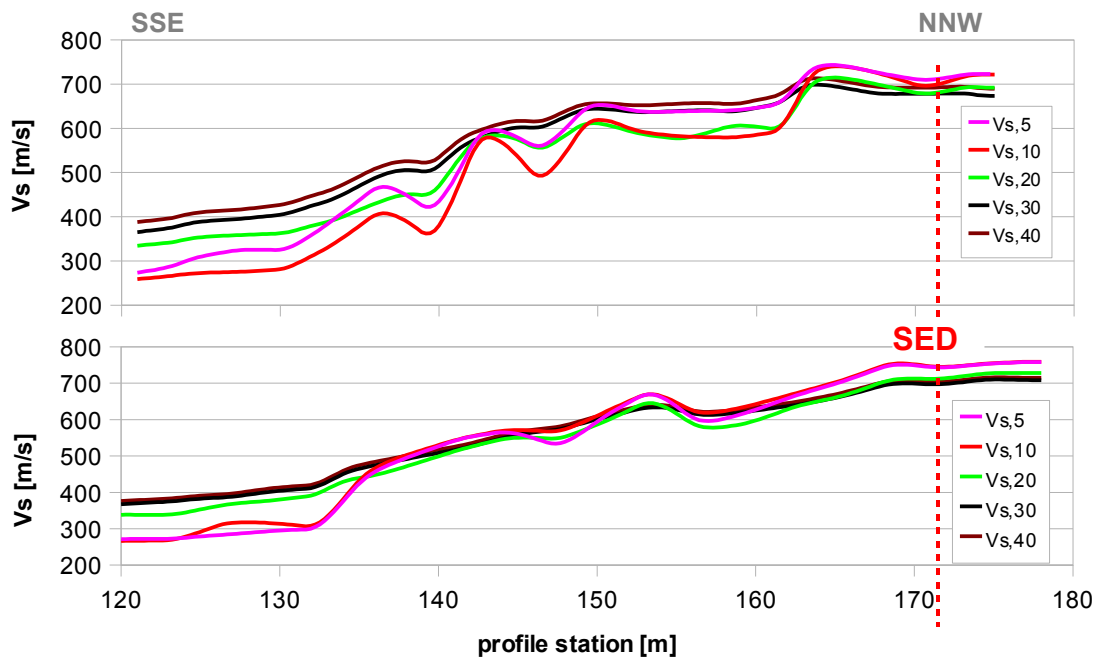v_{si} = corresponding shear-wave velocity.

Fig. 3.3g: *Graphs of the averaged $v_{s,5}$...-values along the profile for the PLUS- (above) and MINUS- (below) directions.*
The station spacing is 1 m, profile meter 0 = profile station 101, profile meter 95 = profile station 196.

The average values of the s-wave velocity model $v_{s,5}$, $v_{s,10}$, $v_{s,20}$, $v_{s,30}$, $v_{s,40}$, $v_{s,50}$, $v_{s,100}$ (= average shear wave velocity from the surface to depths of 5 m, …until 100 m) on the line segment nearest to the SED station (Tab. 3.3c) and at profile station 120 to compare with the former SED own measurements (Tab. 3.3.d) are summarized below:

	Vs,5	Vs,10	Vs,20	Vs,30	Vs,40	Vs,50	Vs,100
MINUS	697	703	662	663	672	n/a	n/a
PLUS	708	687	673	678	693	n/a	n/a
MEAN	703	695	667	670	683	n/a	n/a

Tab. 3.3c: *The average shear wave velocities within the depth intervals from 0 m down to 5 m, etc.… to 100 m, calculated for the line segment with a subjectively most similar geology to the SED station (profile stations 160 to 170).*

	Vs,5	Vs,10	Vs,20	Vs,30	Vs,40	Vs,50	Vs,100
PLUS	279	262	338	369	392	n/a	n/a
PLUS	272	267	338	370	379	n/a	n/a
MEAN	276	264	338	370	385	n/a	n/a

Tab. 3.3d: *The average shear wave velocities within the depth intervals from 0 m down to 5 m, etc.… to 100 m, calculated for the line beginning (profile station 120) to compare with the former SED own measurements.*

3.4 Hybrid Seismic Data Processing

3.4.1 p-wave *Reflection* Seismic Processing Sequence

A) Data conditioning

A1 Reformatting and quality verification of field data
A2 Recording geometry assignment
A3 Data editing (suppression of bad / dead traces, etc.)
A4 Preliminary analysis of refraction velocities

B Filtering and deconvolution

B1 Analytical muting of refraction arrivals
B2 Amplitude recovery / amplitude equalization in time and frequency domains
B3 Predictive deconvolution parameter tests / application
B4 Determination of band limiting corner frequencies / application
B5 Optional 2-D filtering

C) Velocity analysis and stack

C1 Common Depth Point (CDP) sort
C2 Semblance velocity analysis using supergathers of 3 - 5 CDP's
C3 Optional dip move-out correction
C4 Normal Move-Out (NMO) correction and application of stretch mute
C5 Band-pass filtering
C6 CDP stack
C7 Optional coherency filtering

D) Time-depth conversion

D1 Optional spiking deconvolution
D2 Band-pass filtering
D3 Depth conversion
D4 Final display of seismic depth section with inversed polarity (non-SEG-convention)

3.4.2 The presentation of reflection seismic data

The data in a reflection seismic section are presented as an assembly of individual seismic signals at regular intervals along a seismic profile. The simplest way of representing the signals are single wiggle lines (first to the left in the illustration below). A more capturing presentation is the variable area form (second to the left). Combining these two modes results in the var-wiggle mode. Another method of data visualization is the variable density mode (second from the right).

The compressional phase of seismic signals is defined in this report as the onset of the positive amplitude excursion in black (Fig. 3.4a). Since the source signal is produced by an explosion or by an impact at the surface, the signal starts off with a compression of the ground particles. Thus the arrivals of reflection events are defined by the compressional phase.

In rare situations of velocity inversions, cases in which formation velocities are lower than in the layers above, polarity reversals of the reflected signals occur. The beginning of the reflection event would then be characterized by a dilatational phase, represented in this report as a negative amplitude excursion, i.e. in white.
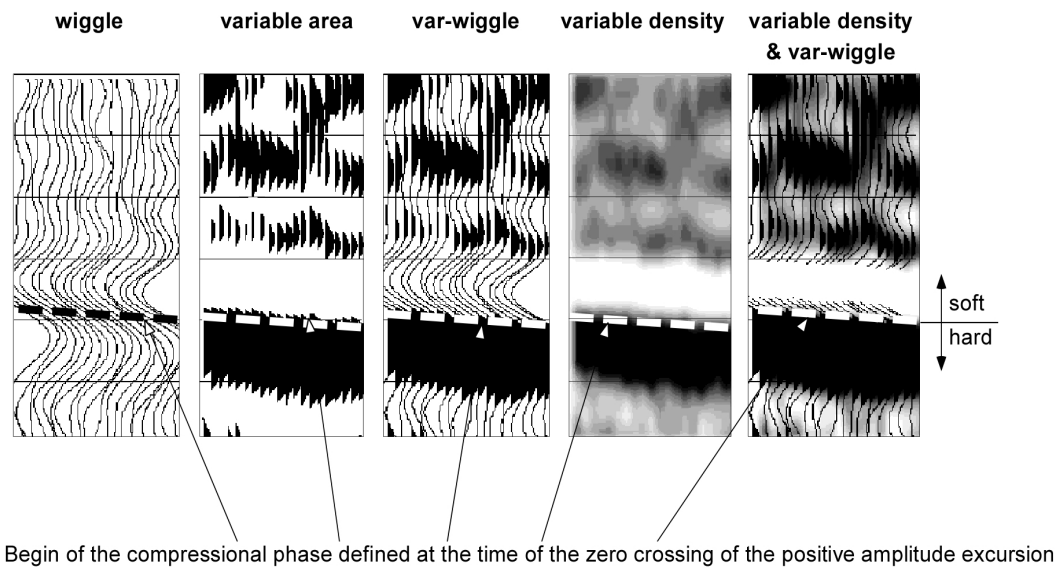
wiggle	variable area	var-wiggle	variable density	variable density & var-wiggle

Begin of the compressional phase defined at the time of the zero crossing of the positive amplitude excursion

Fig. 3.4a   Representation of reflection seismic data and the definition of a reflection event.
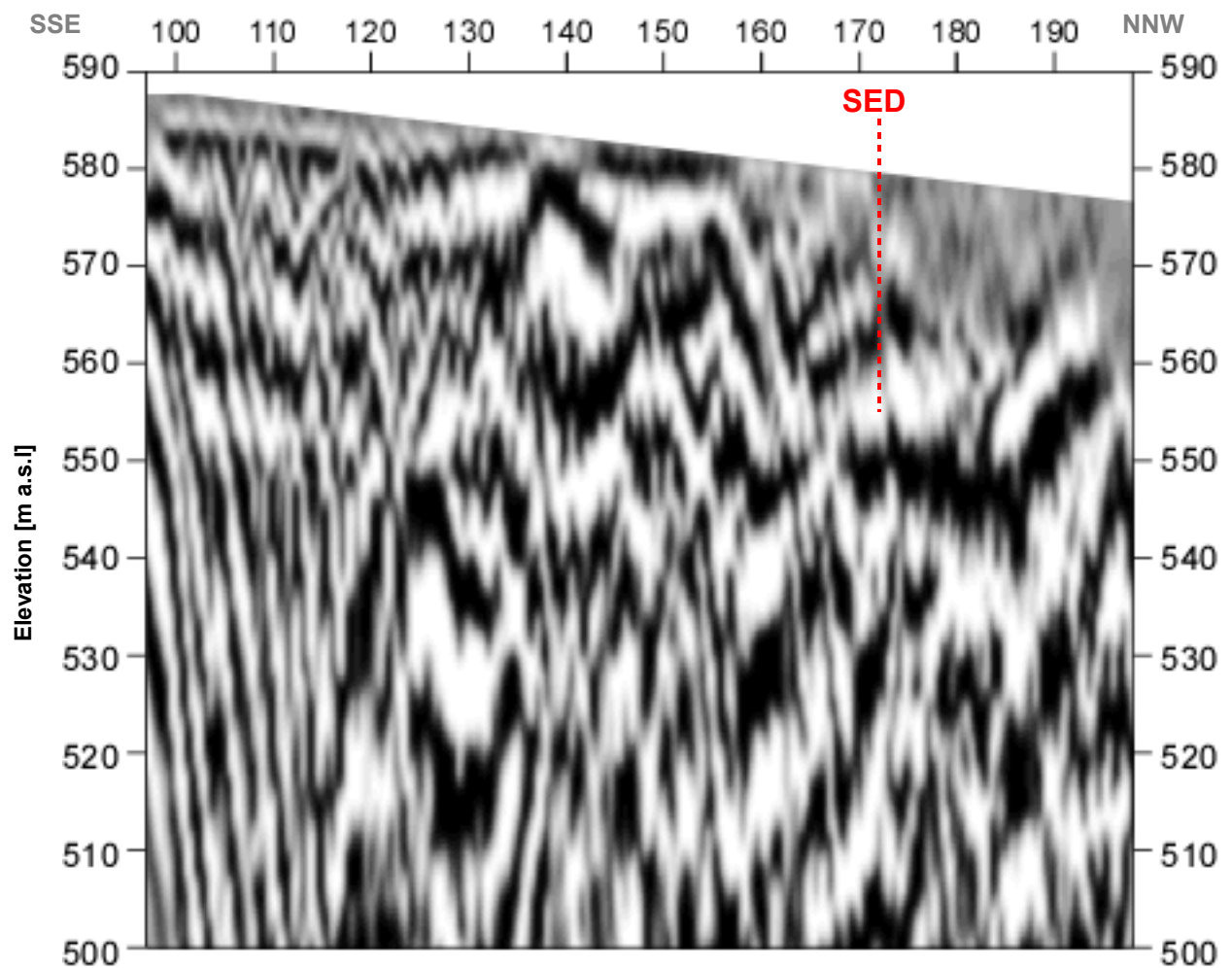

Fig. 3.4b: Seismic depth section with variable density mode.
Vertical axis: elevation [m a.s.l.], horizontal axis: profile meter; no vertical exaggera-
tion. The station spacing is 1 m, profile station 101 = profile meter 0, profile station
196 = profile meter 95.

3.4.3　　p-wave refraction tomography processing

The seismic p-wave refraction processing steps are analogous to those described in paragraph 3.2. For a detailed method statement and a description of the processing steps please refer to the summary report.. The Figs. 3.4c to 3.4g and Tab. 3.4a and 3.4b illustrate the intermediate processing steps and the final result.
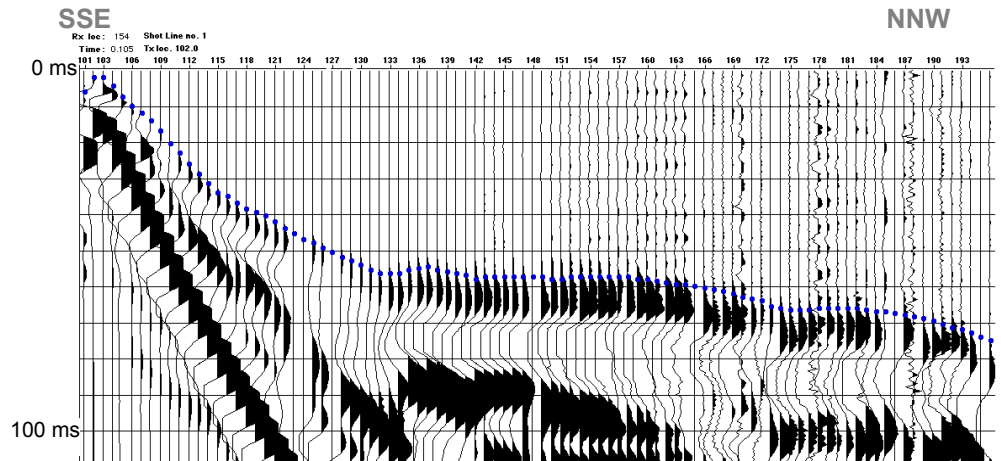

Fig. 3.4c: p-wave record with positive amplitude excursions in black. Blue dots mark the manually picked first break arrival times.
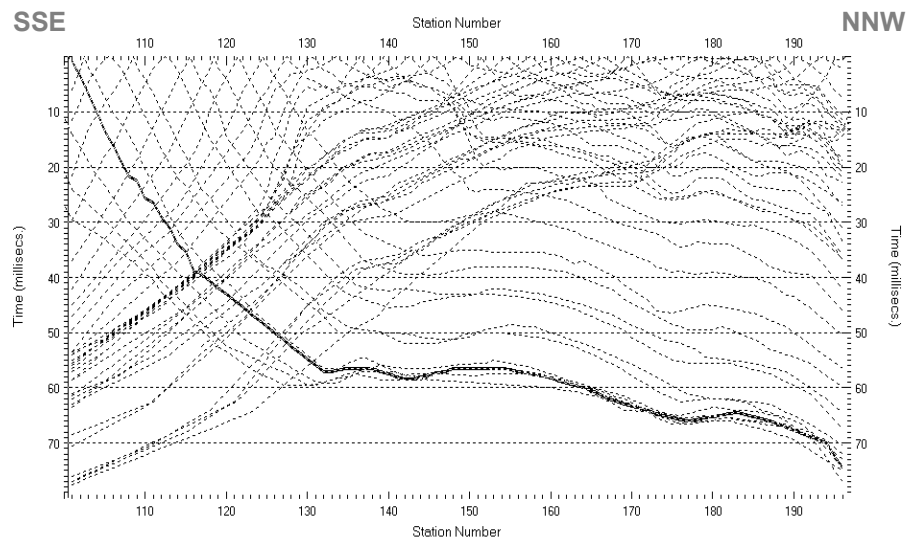*Vertical axis: travel time in ms, horizontal axis: station numbers spaced at 1 m.*

Fig. 3.4d: Travel time curves of p-wave arrival time picks.
The station spacing is 1 m, profile station 101 = profile meter 0, profile station 196 = profile meter 95.

SSE   NNW
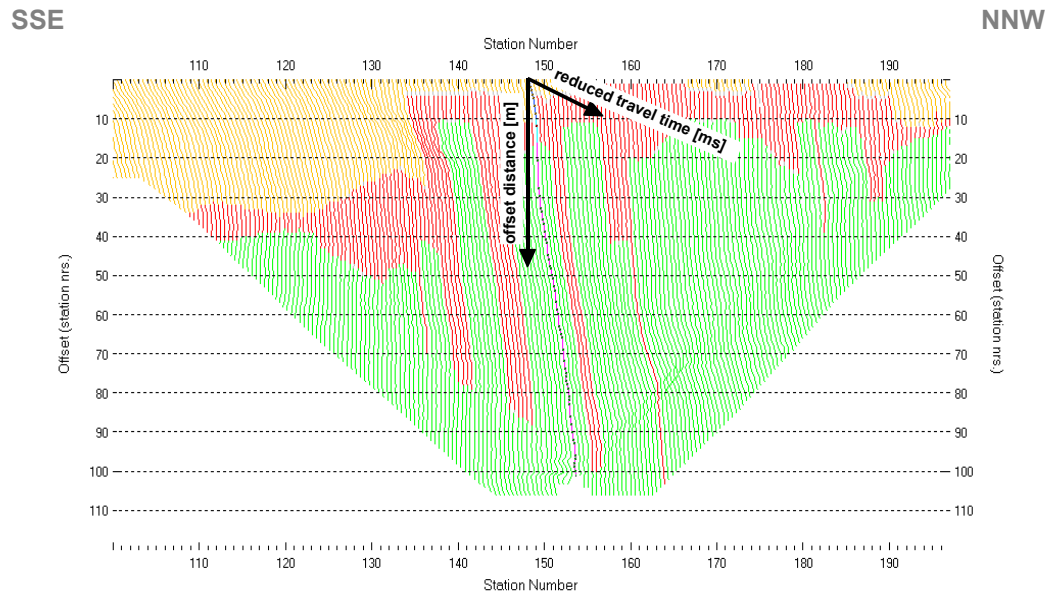

Fig. 3.4e: 3-dimensional distance-travel time diagrams at the mid-points between source points and receiver stations are instrumental when using the analytical CMP derivation of the initial velocity field.
The horizontal axes are along the CMP positions and the travel time respectively, the vertical axis denotes the offset distance between source and receiver positions. The station spacing is 1 m; profile station 101 = profile meter 0; profile station 196 = profile meter 95. The colors represent different velocity layers.

An initial 1D-velocity function (averaged 1D velocity-depth profiles derived by the Delta-t-V method, see Tab. 3.2a) is determined in the 3-dimensional time-offset-CMP-domain from all first break arrival time curves in the 3-dimensional time-offset-CMP-domain (see. Fig. 3.2c).

Depth [m]	Vp [m/s]
0	743
0.2	743
1.87	810
2.79	1182
3.78	1378
7.48	1464
10.66	1600
12.23	1500
13.69	1475
18.31	1553
27.27	1931
31.95	2788
40.56	2556
45.22	2874
60	3189
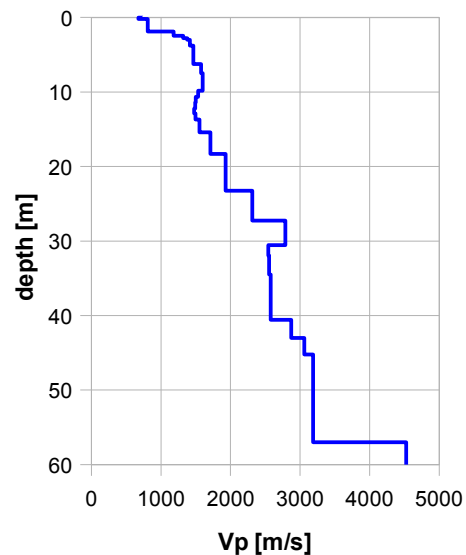
Tab. 3.4a: Initial 1D p-wave velocity model derived from real data. The plotted values are mean values between profile meters 70 and 80 = profile station number 170 and 180.
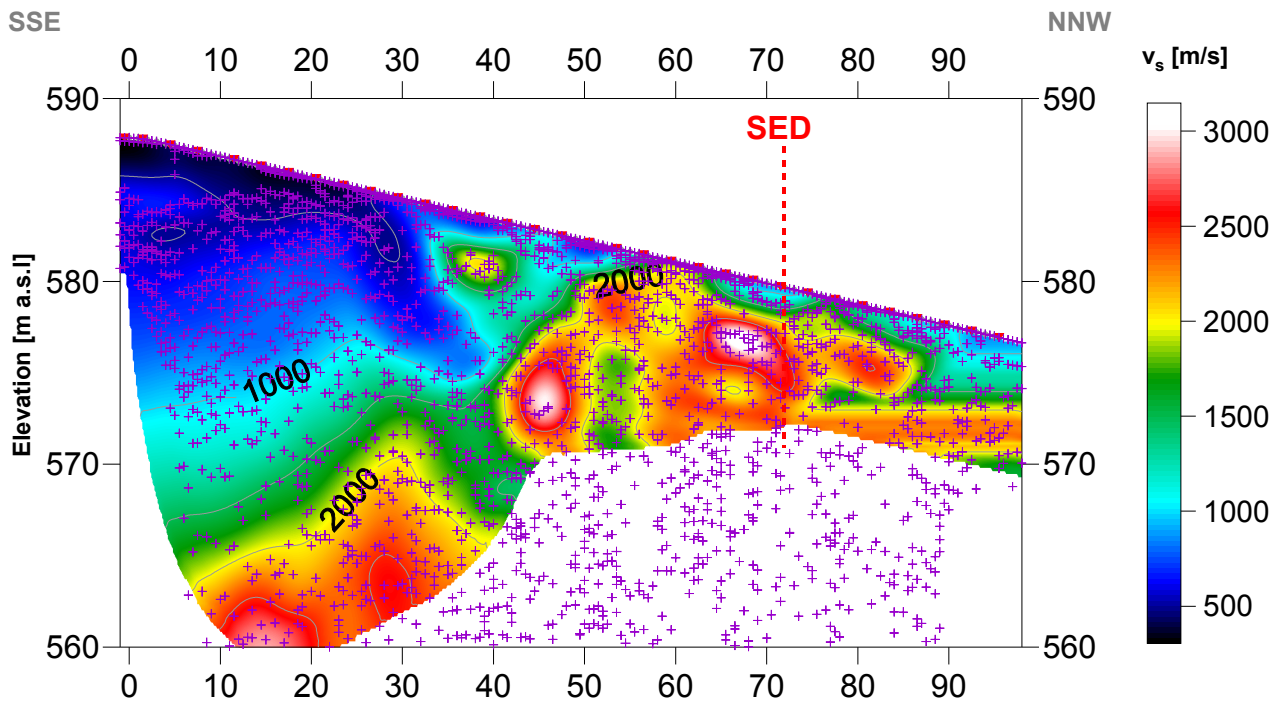
Fig. 3.4f   Compressional wave velocity field image along the seismic profiling. Red/white colors indicate solid rock, blue/black colors unconsolidated sediments and soil.
Vertical axis: elevation [m a.s.l]; horizontal axis: profile meter;color scale: v_s [m/s]; vertical exaggeration: 2:1; gray squares: receiver stations; red triangles: shot positions; magenta crosses: positions of determined velocity values deriving the initial velocity model. The station spacing is 1 m; profile meter 0 = profile station 101; profile meter 95 = profile station 196.

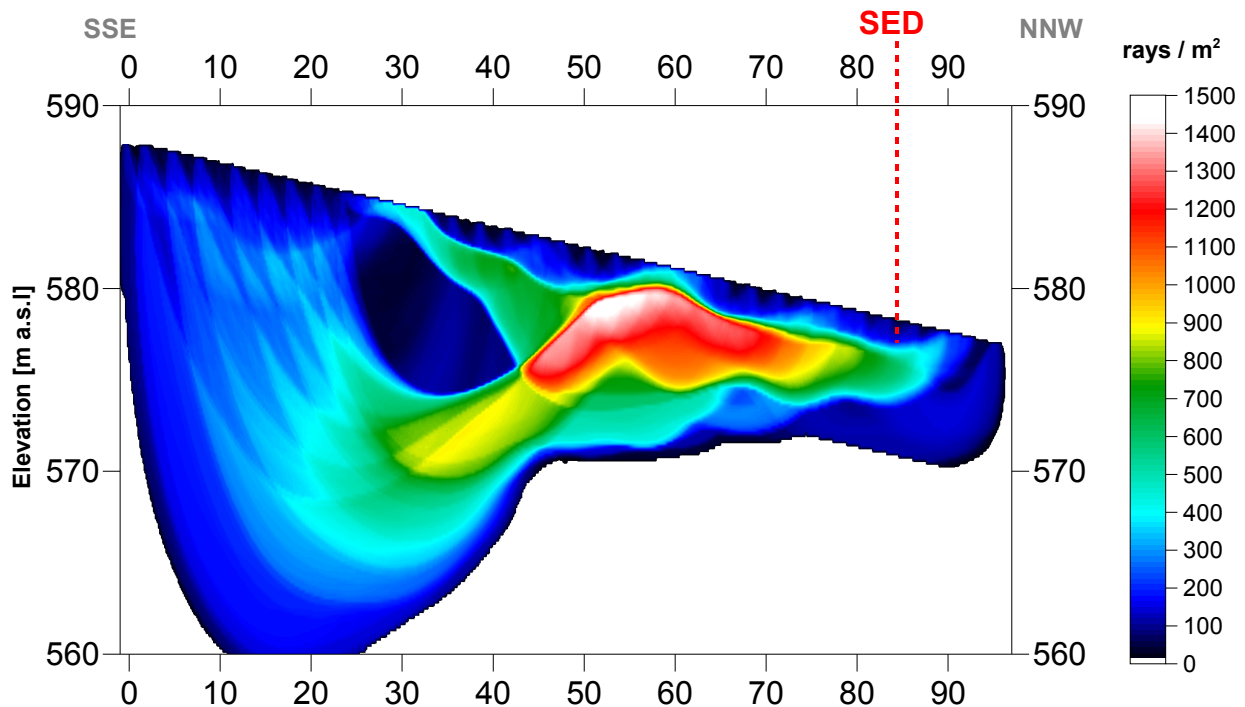Fig. 3.4g   Compressional wave subsurface ray path density along the seismic profile. Red/white colors indicate high velocity contrast between two layers, blue/black colors low coverage areas.
Vertical axis: elevation [m a.s.l]; horizontal axis: profile meter; color scale: ray paths per m²; vertical exaggeration: 2:1. The station spacing is 1 m; profile meter 0 = profile station 101; profile meter 95 = profile station 196.

The final velocity model at the SED station derived from the p-wave dataset in Tab. 3.4b gives values down to less than 10 m depth. The reason for this small amount is due to the seismic refraction method: when the velocity changes in a medium are small, a seismic ray does not refract inside the medium. So no informations can be calculated from that depth.

Depth [m]	Vp [m/s]
0.0	933
0.7	1234
1.2	1549
1.8	1786
2.3	1937
2.8	2083
3.3	2260
3.8	2374
4.3	2391
4.8	2352
5.3	2263
5.8	2109
6.3	2012
6.8	2110
7.3	2255
7.8	2315
8.3	2293
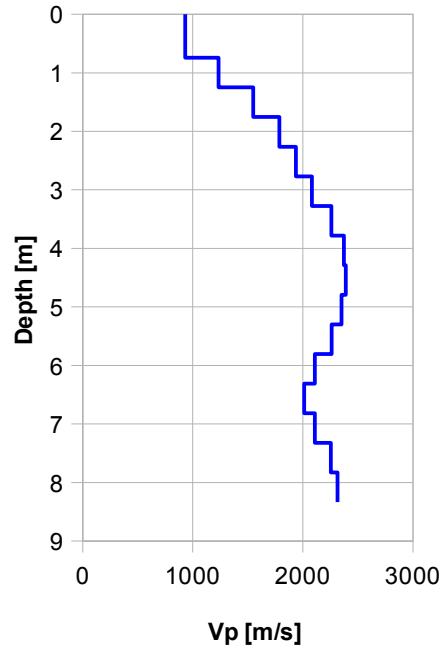
Tab. 3.4b: *Final 1D p-wave velocity model derived from real data (horizontal average of all values) at a position most similar to the geological setting at SED station between profile meters 70 and 80 = profile station number 170 and 180.*

3.4.4 Representation of the hybrid seismic section

The hybrid seismic section is the reflection seismic section with the superimposed p-wave velocity field. It portrays the geological structures and the p-wave velocity field, the latter being indicative for the rock / soil rigidity. The uninterpreted hybrid seismic section is portrayed in Fig. 3.4h below.
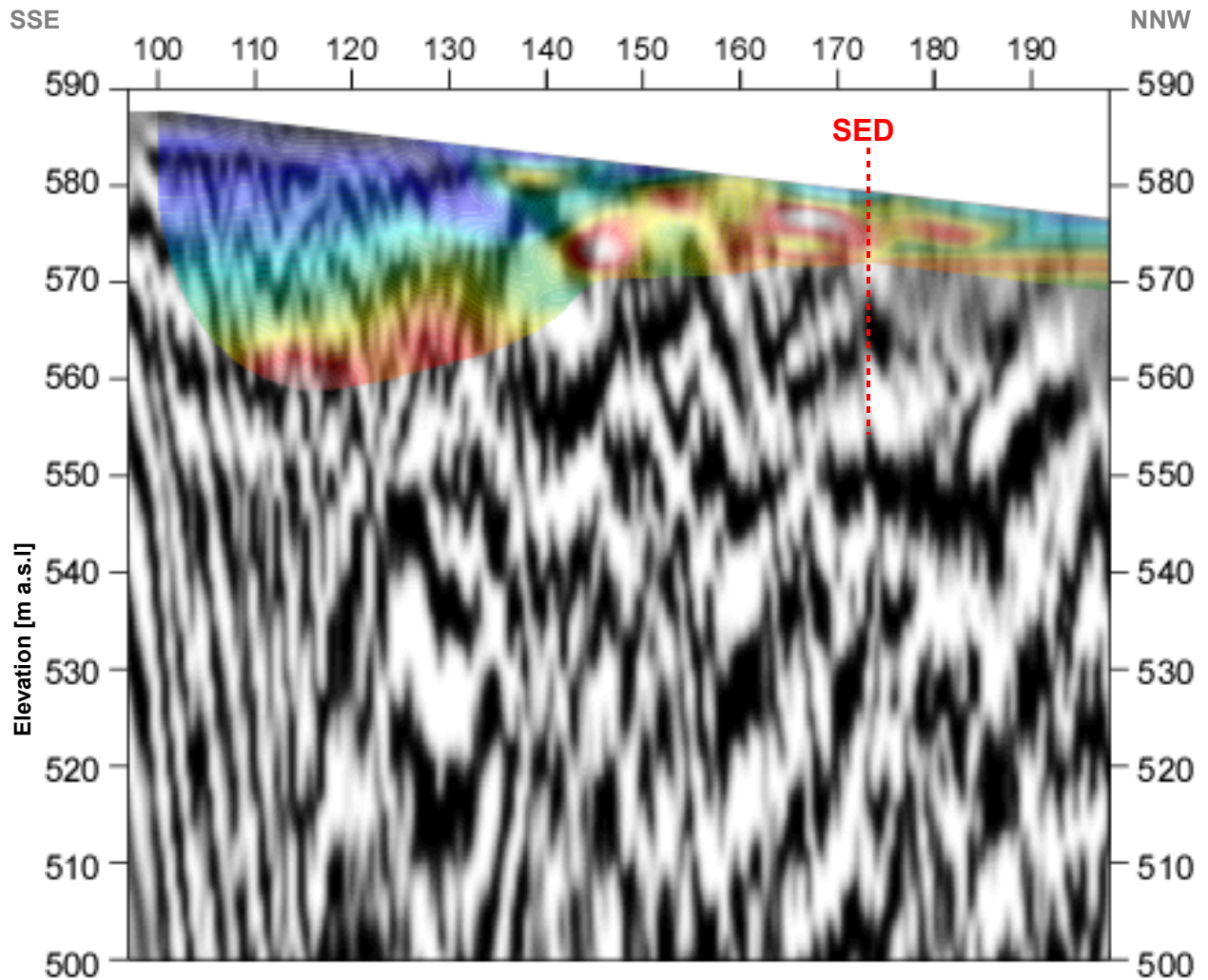

Fig. 3.4h   *Uninterpreted hybrid seismic section: superimposed onto the seismic reflection section is the color encoded p-velocity field derived by refraction tomography.*
No vertical exaggeration. The station spacing is 1 m, profile station 101 = profile meter 0; profile station 196 = profile meter 95.

4 DISCUSSION OF THE RESULTS

4.1 Summary of the Results

Compressional and shear wave velocity data from refraction seismic surveys both p-wave and s-wave and also the MASW survey data from profile 09SN_14SLE-1 are shown in Tab. 4.1 for the uppermost 10 m. The theoretical shear wave velocity $v_{s(calc)}$ in Tab. 4.1 was calculated by a theoretical v_p/v_s-ratio of $\sqrt{3}$.

Depth	Vp measured	Vs measured	Vs calculated	Vs MASW
0.0	933	783	538	694
0.7	1234	904	712	
1.2	1549	1173	895	699
1.8	1786	1191	1031	
2.3	1937	1214	1118	697
2.8	2083	1273	1203	
3.3	2260	1455	1305	
3.8	2374	1631	1370	678
4.3	2391	1663	1380	
4.8	2352	1574	1358	
5.3	2263	1453	1307	
5.8	2109	1384	1218	655
6.3	2012	1383	1162	
6.8	2110	1466	1218	
7.3	2255	1595	1302	
7.8	2315	1746	1337	
8.3		1925		641
8.8		2117		
9.3		2342		
9.9				
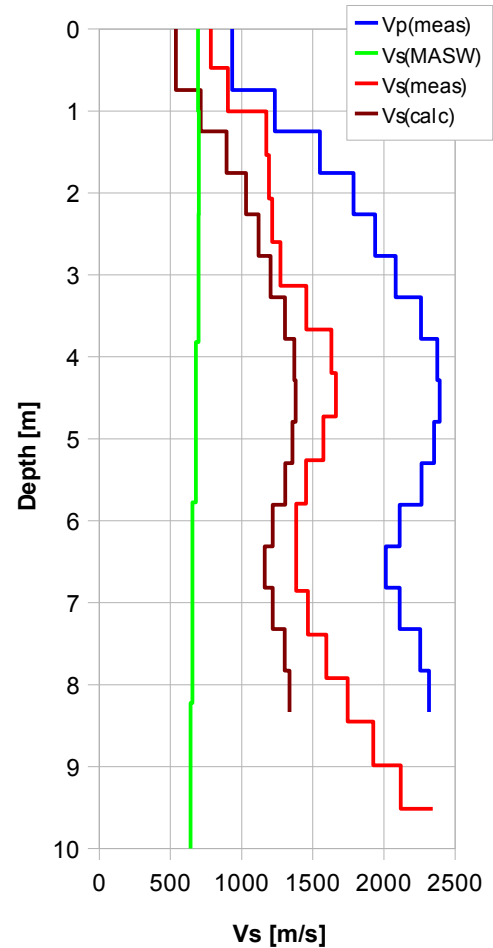
Tab. 4.1: Shear and compressional wave velocities determined at a distance of 25 m from the SED station SLE.

Fig. 4.1: Graphic display of shear and compressional wave velocities determined at a distance of 25 m from the SED station SLE.

Differences between calculated v_s and observed v_s in Tab. 4.1 possibly occur because of converted waves (shear wave to compressional wave to shear wave on layer boundaries, i.e. soil – unconsolidated sediments or unconsolidated sediments – hard rock).

4.2 Validation of the methods and their results

Due to methodological differences, v_s velocities derived by MASW analysis resp. refraction technique may differ much. This is because MASW analysis cannot show small inhomogeneities as a dispersion image with a array length of i.e. 40 m gives only one value at each depth. On the other hand, refraction derivation has a high lateral resolution but is limited with depth information. The interpretation of the refraction velocity values must be held with caution due to possible wave conversions at layer boundaries.

4.3 Error Estimates

The error estimates given in Tab. 4.3 below, being strongly influenced by the geological complexity of the investigated area, are relevant only in the context of this survey.

Surveying method	Type of result	Error estimate
v_s – refraction tomography	v_s – velocity field image	15%*
MASW only "+" or only "-" values	v_s – velocity field image	20%
MASW (mean of "+" & "-" values)	v_s – velocity field image	10%
v_p – refraction tomography	v_p – velocity field image	10%
Reflection seismic surveying	Image of subsurface structures	n.a.

Tab. 4.2   Error estimates for the methods applied. Note that higher error estimates are to be taken into account with increasing depths.
*v_s values may be determined from converted seismic waves which denote always too high velocities.

The above error estimates are of a qualitative character only. In view of the intense fluctuations to be expected in both the lateral and vertical directions, any attempt to derive a quantitative general error estimate to be valid for the entire survey is to be considered as futile.

Furthermore, the error estimates for the MASW method depend to a great extent on the experience of the processing geophysicist. As compared to the refraction tomography techniques, substantially more subjective decision making is required while processing MASW data.

At the SED station SLE (Schleitheim), the refraction velocity images both from shear and compressional wave analysis show coincident structures. The MASW values seems to be generally too low for calcareous rocks where the refraction shear wave velocities seems to be derived (partly) from converted waves, so these values are too high.

4.4 The Geophysical Interpretation

The most conclusive information about the subsurface structures is provided by the results of the hybrid seismic section (v_p-refraction tomography profiling and reflection seismic section) and confirmed by the evaluation findings of the v_s-refraction tomography data.

As can be seen from the v_s and v_p refraction tomography sections in Fig. 3.2d & Fig. 3.4f, the topography of the bedrock surface is clearly imaged in great detail on the NNW half of the profile. At profile station 160 (=profile meter 60) the bedrock outcrops at the surface, and at the NNW end of the profile, the thickness of the loose material overburden is a max. of 2 m.

Between profile stations 160 and 140 the depth of bedrock surface increases to about 7 m. To the SSE of station 140, it steeply dips to a depth of at least 20 m below the surface. At the SSE end of the profile the extrapolated bedrock depth is about 30 m below the surface.

Contrary to the regular layering observed at bedrock outcrop in the wall behind the SED monitoring station, the reflection seismic section in Fig. 3.4b reveals a highly irregular pattern of the internal bedrock structures as is evidenced by numerous diffraction events.
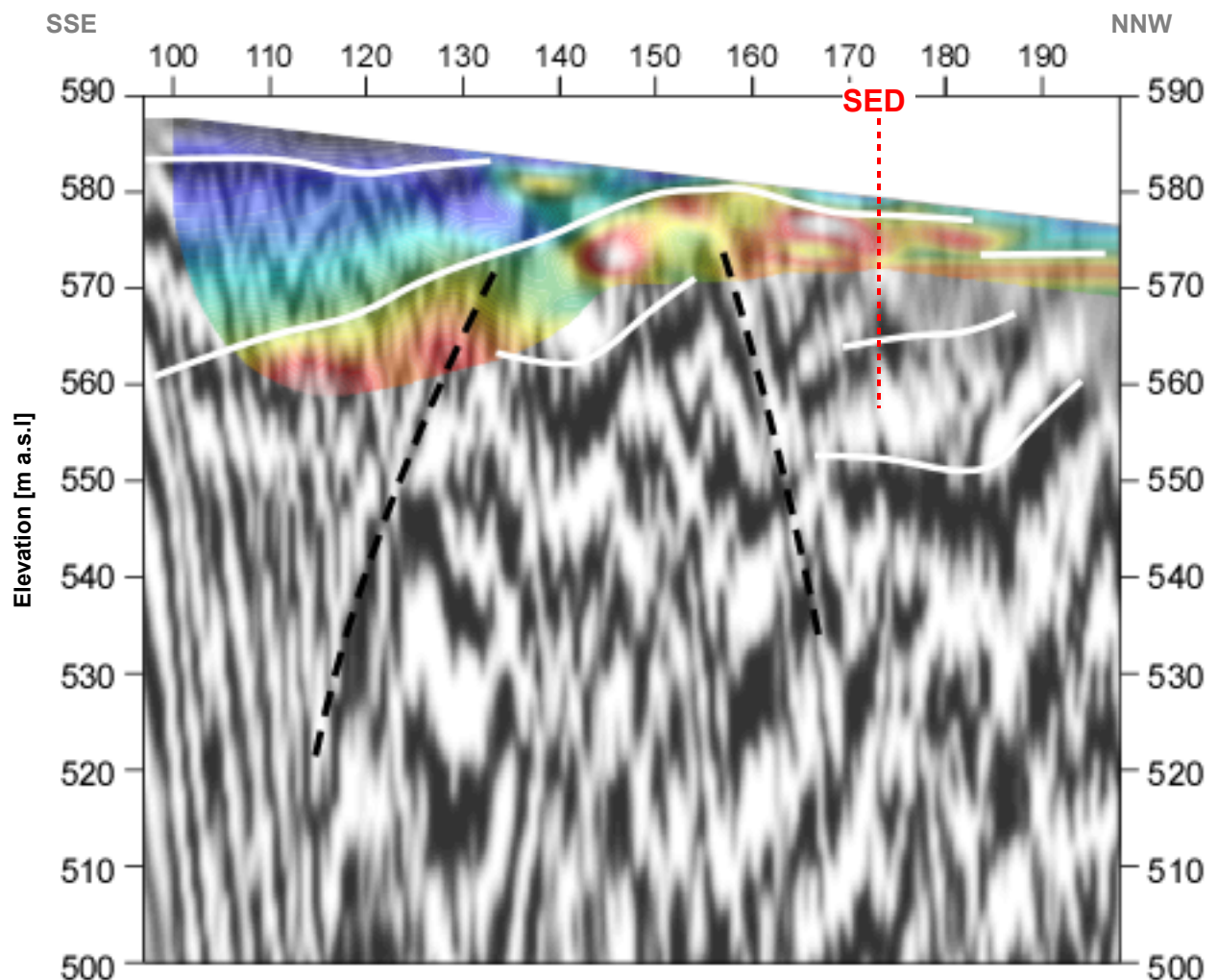

Fig. 4.2: *Geophysical interpretation of the hybrid seismic section. In grayscale is the seismic reflection section with the superimposed color encoded the p-wave velocity field. White lines denote layer boundaries; black dotted lines are indicative of suspected faulting.*
No vertical exaggeration. The station spacing is 1 m, profile station 101 = profile meter 0; profile station 196 = profile meter 95.

5 SUMMARY AND CONCLUSIONS

- In December 2008 a combined seismic s- and p-wave survey was carried out at the SED earthquake monitoring station SLE near Schleitheim SH.

- The shear wave data have been evaluated by conventional diving wave refraction tomography techniques in order to derive the s-wave velocity field along the seismic line. Due to the inherent constraints of the refraction tomography method, the depth of investigation is limited to 15 m under the prevailing geological conditions.

- The p-wave have been processed

  - to derive a 2D s-wave velocity field by using the MASW (**M**ultichannel **A**nalysis of **S**urface **W**aves) technique;

  - and secondly, according to the hybrid seismic data processing scheme for representing the subsurface structures in a combined reflection seismic section with the superimposed p-wave velocity field.

- The shear wave velocity range determined by MASW method in the uppermost 30 meters spans from values of 233 m/s to 992 m/s. Pronounced velocity variations along the seismic line point to highly heterogeneous structures in the subsurface:

  - At the southern end of the line, the bedrock surface is situated at a depth of at least 20 m. The material in the overburden consists of top soil and disintegrated weathered rock with s-wave velocities of up to 500 m/s.

  - On the NNW half of the line, the bedrock is close to the surface. Here, the s-wave velocity for the bedrock at a depth of 10 m is found to be between 800 m/s and 1400 m/s.

  - At the northern end of the profile, at the rim of the quarry, s-wave velocities in the range of 800 m/s have been found in the top layer of the subsurface.

- The scalar values derived by the MASW survey at SED station SLE (seismic profile 09SN_14SLE-1, profile station 165) are the following:

  $v_{s,5}$ = 703 m/s
  $v_{s,10}$ = 695 m/s
  $v_{s,20}$ = 667 m/s
  $v_{s,30}$ = 670 m/s
  $v_{s,40}$ = 683 m/s
  $v_{s,50}$ = n/a

- The maximal determined refraction shear wave velocity is 1663 m/s in 4.2 m resp. compressional wave velocity is 2391 m/s below 4.3 m depth.

- The geophysical interpretation of the subsurface structures in this report are to be validated and incorporated into a comprehensive appraisal by a geologist familiar with the local geological setting.

Schwerzenbach, 24th March 2009

Walter Frei
dipl. Natw. ETH
managing director

Lorenz Keller
dipl. Natw. ETH
project manager